

ENERGY LOSS AND SCATTERING OF SUBEXCITATION ELECTRONS IN SiO₂[†]

J. C. Ashley, R. H. Ritchie, and O. H. Crawford
 Health and Safety Research Division
 Oak Ridge National Laboratory
 Oak Ridge, TN 37831-6123, USA

CONF-870155--2

Introduction

DE87 006619

For electrons with energies below the band gap energy of ~9 eV in SiO₂, energy loss or gain occurs through phonon emission or absorption. Coupling to the longitudinal optical (LO) modes has been considered by several workers in connection with "electron-runaway" and subsequent "breakdown" when high electric fields are applied to this insulator.¹⁻³ The important role played by acoustic phonon modes in predicting the breakdown field in SiO₂ was recently discussed by Fischetti⁴ and Fischetti, et al.⁵ following the theoretical formulations described by Sparks, et al.⁶ We have re-examined these interactions and evaluated the energy loss per unit pathlength and transport mean free path to aid in a qualitative description of the behavior of subexcitation electrons in SiO₂. For example, energy losses and angular deflections experienced by subexcitation electrons in matter are very important in establishing whether geminate recombination occurs between an ejected electron and its parent ion in radiation physics. The response of solid-state devices to ionizing radiation is determined in part by recombination processes, which in turn may depend importantly on the kinds of cross sections that we consider here.

Interaction with LO Modes

For interaction with the LO modes we use the Frölich model⁷ as described by Llacer and Garwin⁸ and by Fitting and Friemann.³ The contribution to the stopping power from a single LO mode for an electron with speed v and energy E is given by

$$-\frac{dE}{dx} \Big|_{LO} = \frac{e^2 \omega^2}{v^2} \left(\frac{1}{\epsilon_\infty} - \frac{1}{\epsilon_0} \right) \left\{ (n_\omega + 1) \ln \left(\frac{W_2^+}{W_1^+} \right) - n_\omega \ln \left(\frac{W_2^-}{W_1^-} \right) \right\} \quad (1)$$

where

$$W_2^\pm = \min \left\{ k \left(1 + \sqrt{1 \mp \hbar\omega/E} \right), k_{BZ} \right\}$$

$$W_1^\pm = \pm k \left(1 - \sqrt{1 \mp \hbar\omega/E} \right)$$

$$m^* v = \hbar k = \sqrt{2m^* E}$$

$$k_{BZ} = (6\pi^2/V_p)^{1/3}$$

[†]The submitted manuscript has been authored by a contractor of the U.S. Government under contract No. DE-AC05-84OR21400. Accordingly, the U.S. Government retains a nonexclusive, royalty-free license to publish or reproduce the published form of this contribution, or allow others to do so, for U.S. Government purposes.

MASTER

$$n_{\omega} = \left[\exp(\hbar\omega/k_B T) - 1 \right]^{-1}.$$

Here V_p is the volume of the primitive cell, $\hbar\omega$ is the LO phonon energy, $k_B T$ is the thermal energy of the lattice, and m^* is the electron effective mass. The transport mean free path is given by

$$\lambda_{t,LO}^{-1} = \lambda_{t+}^{-1} + \lambda_{t-}^{-1}$$

where

$$\lambda_{t\pm}^{-1} = \frac{e^2 \omega}{\hbar v^2} \left[\frac{1}{\epsilon_{\infty}} - \frac{1}{\epsilon_0} \right] \left[n_{\omega} + \frac{1}{2} \pm \frac{1}{2} \right] \int_{W_1^{\pm}}^{W_2^{\pm}} \frac{dq}{q} (1 - \cos\theta_{\pm}) \quad (2)$$

and the scattering angle θ_{\pm} for phonon emission (+) or absorption (-) is determined from conservation of energy and momentum. We find

$$\lambda_{t\pm}^{-1} = \frac{e^2 \omega}{\hbar v^2} \left[\frac{1}{\epsilon_{\infty}} - \frac{1}{\epsilon_0} \right] \left[n_{\omega} + \frac{1}{2} \pm \frac{1}{2} \right] \left\{ \left[1 - \frac{1 + \hbar\omega/2E}{(1 + \hbar\omega/E)^{1/2}} \right] \ln(W_2^{\pm} / W_1^{\pm}) + \frac{(W_2^{\pm})^2 - (W_1^{\pm})^2}{4k^2(1 + \hbar\omega/E)^{1/2}} \right\}. \quad (3)$$

The scattering rate is given by

$$\tau = \frac{e^2 \omega}{\hbar v} \left[\frac{1}{\epsilon_{\infty}} - \frac{1}{\epsilon_0} \right] \left[(n_{\omega} + 1) \ln(W_2^+ / W_1^+) + n_{\omega} \ln(W_2^- / W_1^-) \right] \quad (4)$$

$$\equiv \tau_{em} + \tau_{abs}$$

with the abbreviations "em" for phonon emission and "abs" for phonon absorption.

For SiO_2 ("ordinary low-temperature quartz") we have⁹ $V_p = 112.98 \text{ \AA}^3$ or 762.3 au where au means atomic units ($\hbar=m=e=1$). This value implies $k_{BZ} = .4267$ au so $E_{BZ} = \hbar^2 k_{BZ}^2 / 2m^* = 2.48$ eV with $m^* = 1$ au. Each primitive cell contains 3 SiO_2 molecules so the average volume per molecule is $V_p/3$. This number is the same as the average volume per molecule assuming a density of 2.65 g/cm^3 . For the electron effective mass take⁶

$$m^*/m = \begin{cases} 1/2, & E \leq E_{BZ}/2 \\ E/E_{BZ}, & E_{BZ}/2 < E < E_{BZ} \\ 1, & E \geq E_{BZ} \end{cases}$$

All results are calculated for "room temperature," $k_B T = .025$ eV.

The strength of the LO mode is proportional to $1/\epsilon_\infty - 1/\epsilon_0$ where ϵ_0 is the static dielectric constant and ϵ_∞ is the dielectric constant in the optical region below the onset of UV absorption. For alkali halides with a single LO mode, the above equations can be applied directly; for SiO_2 there are several prominent LO modes. The division of the mode strengths can be made from the infrared data of Spitzer and Kleinman.¹⁰ The energy-loss function, $\text{Im}(-1/\epsilon)$, for SiO_2 is shown in Fig. 1 as a function of wavenumber $\tilde{\nu}$ as determined from fitting parameters in Table I(a) and Eq. (1) of Ref. 10. Of the several LO modes present, the two considered most important¹⁻³ occur at $\tilde{\nu} = 508.3 \text{ cm}^{-1}$ (0.063 eV) and $\tilde{\nu} = 1237 \text{ cm}^{-1}$ (0.1534 eV). Since

$$\frac{1}{\epsilon_\infty} - \frac{1}{\epsilon_0} = \frac{2}{\pi} \int_0^{\tilde{\nu}_\infty} \frac{d\tilde{\nu}}{\tilde{\nu}} \text{Im}(-1/\epsilon), \quad (5)$$

where $\tilde{\nu}_\infty$ is a value of $\tilde{\nu}$ for which $\epsilon = \epsilon_\infty$, and taking 900 cm^{-1} as the separation point, the strengths of the two modes are found from Eq. (5) to be

$$\left[\frac{1}{\epsilon_\infty} - \frac{1}{\epsilon_0} \right]_{.063} = \frac{2}{\pi} \int_0^{900} \frac{d\tilde{\nu}}{\tilde{\nu}} \text{Im}(-1/\epsilon) = .08104$$

$$\left[\frac{1}{\epsilon_\infty} - \frac{1}{\epsilon_0} \right]_{.1534} = \frac{2}{\pi} \int_{900}^{2500} \frac{d\tilde{\nu}}{\tilde{\nu}} \text{Im}(-1/\epsilon) = .1124$$

These numbers can be compared with values in Ref. 5 of .063 and .143 (only the latter number can be found in Ref. 1, the purported source). The total strength .193 is slightly smaller than the .206 of Ref. 5 but larger than the value .181 used in Ref. 3.

The scattering rate will be described first since other calculations are available for comparison. Scattering rates for emission and absorption calculated from the constants described above are shown in Fig. 2. The total scattering rate calculated with $m^*/m = 1$ for all electron energies, and with mode strengths of Ref. 5, agrees well with predictions given in Fig. 5 of Ref.

5. Comparison of $m^*/m = 1$ results with Fig. 1 in the Fitting and Friemann paper (Ref. 3) show that they use the ~~same~~ strength, .181, for each mode and thus overestimate the total scattering rate. We find γ (10^{15} sec^{-1}) at .4 eV (near the maximum) is .49 (with $m^*/m = 1$) and .70 ($m^*/m = 1/2$) compared with the Fischetti value of $\sim .6$ and the Fitting and Friemann value of $\sim .8$.

The energy loss per unit pathlength due to energy loss to (and gain from) LO phonons is shown in Fig. 3. The small increase in energy loss rate for $T = 0^\circ \text{ K}$ can be seen only in the contributions from the low energy mode as shown by the dashed curves. For $E \gtrsim .17 \text{ eV}$, increases are much less than 1 percent.

The transport mean free path, calculated from Eq. (3), is shown in Fig. 4 as λ_t^{-1} versus electron energy. The "acoustical" curve will be discussed later.

Interaction with Acoustical Modes

Our description of the interaction of an electron with acoustical modes follows the treatment outlined by Sparks, et al.,⁶ as applied to SiO_2 by Fischetti.^{4,5} Considerable uncertainty is present in these calculations due to a variety of approximations as discussed in Refs. 4-6. We start with the scattering rate for acoustic phonon emission (+) or absorption (-) given by

$$\gamma^\pm = \frac{3|S|^2}{4\pi M_p N_c \hbar v} \int_0^{q_{\text{max}}^\pm} dq \frac{q^3}{\omega(q)} \left[n(q) + \frac{1}{2} \pm \frac{1}{2} \right] f(q) \quad (6)$$

where we have assumed the three acoustic modes will be treated as equivalent with sound velocity C_s . The matrix element $S(q) = S$ is assumed to be constant for all q . Variation of the mass M from the mass of the primitive cell, M_p , for small q , to the mass of the heaviest constituents for $q \gtrsim k_{\text{BZ}}$ is incorporated through

$$\frac{1}{M} = \frac{1}{M_p} f(q) \equiv \frac{1}{M_p} (1 + Cq^2)$$

Further definitions and assumptions are:

N_c = density of primitive cells

$$\omega(q) = \begin{cases} C_s q & , q < k_{\text{BZ}} \\ C_s k_{\text{BZ}} & , q \geq k_{\text{BZ}} \end{cases}$$

$$\hbar k = m^* v = \sqrt{2m^* E}$$

$$q_{\max}^{\pm} = \begin{cases} 2k \mp 2m^* C_s / \hbar & , \quad q < k_{BZ} \\ k \left[1 + \sqrt{1 \mp \hbar C_s k_{BZ} / E} \right] & , \quad q \geq k_{BZ} \end{cases}$$

$$n(q) = \begin{cases} \left[e^{\alpha q} - 1 \right]^{-1} & , \quad q < k_{BZ} \\ \left[e^{\alpha k_{BZ}} - 1 \right]^{-1} & , \quad q \geq k_{BZ} \end{cases}$$

$$\alpha \equiv \hbar C_s / k_B T$$

The energy loss per unit pathlength, or the contribution to the stopping power of the medium due to interaction with the acoustic modes is

$$-\frac{dE}{dx} = \frac{3|S|^2}{4\pi M_p N_c v^2} \left\{ \int_0^{q_{\max}^+} dq q^3 f(q) - \int_{q_{\max}^+}^{q_{\max}^-} dq q^3 f(q) n(q) \right\} \quad (7)$$

The transport mean free path is calculated from

$$\begin{aligned} 1/\lambda_t = & \frac{3|S|^2}{4\pi M_p N_c \hbar v^2} \left\{ \int_0^{q_{\max}^+} dq \frac{q^3}{\omega(q)} f(q) [n(q)+1] (1-\hat{k} \cdot \hat{k}')_+ \right. \\ & \left. + \int_0^{q_{\max}^-} dq \frac{q^3}{\omega(q)} f(q) n(q) (1-\hat{k} \cdot \hat{k}')_- \right\} \quad (8) \end{aligned}$$

where

$$(\hat{k} \cdot \hat{k}')_{\pm} = \frac{1 - q^2 / 2k^2 \mp \hbar \omega(q) / 2E}{\sqrt{1 \mp \hbar \omega(q) / E}}$$

and, again, the top sign corresponds to phonon emission by the electron and the bottom sign corresponds to absorption of a phonon by the electron.

The parameters for SiO₂ for these calculations are $V_p = 762.3$ au, $N_c = 1/V_p = 1.312 \times 10^{-3}$ au, $k_{BZ} = .4267$ au, and $E_{BZ} = 2.48$ eV. For $f(q)$, M_p

is the mass of 3 SiO₂'s while M is the mass of 3 silicon atoms for $q \geq k_{BZ}$, so $f(k_{BZ}) = 2.139$ and $C = 6.256$. The "average" sound velocity is calculated from $C_T = 3.75 \times 10^5$ cm/s and $C_L = 5.90 \times 10^5$ cm/s through $3/C'_s = 2/C_T + 1/C_L$ for "clear, fused quartz" with $\rho = 2.2$ g/cm³. Scaling to $\rho = 2.64$ g/cm³ through $C_s = C'_s (2.2/2.64)^{1/2}$ gives $C_s = 1.79 \times 10^{-3}$ au. $S = 3.5$ eV from Refs. 4 and 5.

The scattering rate for interaction with acoustic phonons, $\gamma_{ac} = \gamma^+ + \gamma^-$, calculated from Eq. (6), is shown in Fig. 5 along with the total scattering rate for interaction with LO phonons. The scattering rate γ_{ac} can be compared with Fischetti's result,⁴ a portion of which is shown by the dashed curve in our Fig. 5. At 6 eV we predict 3.2 compared with 3.6 from Ref. 4 or 5. Since the energy dependence should be the same for both calculations, the curves should remain parallel for $E > 6$ eV. For $E \gtrsim 3$ eV, our curve is given approximately by

$$\gamma_{ac} \approx 0.22 [E(\text{eV})]^{1.5} .$$

The most obvious difference in the two results for γ_{ac} is in the location of the "kinks" in the curves at $E_{BZ}/2$ and E_{BZ} , since Fischetti used a value for E_{BZ} twice as large as ours.

Both γ , Fig. 5, and $1/\lambda_t$, Fig. 4, are dominated at the higher energies by interactions with the acoustic phonons. While contributions to $1/\lambda_t$ from acoustic and LO phonons are of the same order of magnitude for $E \lesssim 1$ eV, the stopping power (Fig. 3) is determined almost totally by LO phonons due partly to the smaller average acoustic phonon energy. These features are manifest in Monte Carlo trajectory simulations of electrons accelerated by small and large values of electric field (Ref. 5, Fig. 12). At small fields the transport is influenced mainly by forward, LO scattering while at high fields scattering by acoustic modes dominates (small λ_t), i.e. many large-angle scattering events, increasing the pathlength and thus the probability of energy loss to the LO modes.

As an additional example of the use of this information in studying the behavior of subexcitation electrons, we calculate the mean square pathlength traveled by an electron in slowing down from an energy equal to the bandgap energy, $E_G \approx 9$ eV, to an energy E . It is determined from the energy loss per unit distance and the transport mean free path through

$$\overline{r^2}(E) = 2 \int_E^{E_G} \frac{dE'}{\lambda_t^{-1}(E') \left[-\frac{dE'}{dx}(E') \right]} . \quad (9)$$

The results are shown in Fig. 6. The root-mean-square pathlength, $[\overline{r^2}(E)]^{1/2}$, for slowing to 1 eV is $\sim 190 \text{ \AA}$ while slowing to $E = 0.1 \text{ eV}$ gives $\sim 220 \text{ \AA}$. At electron energies below $\sim 0.06 \text{ eV}$, the energy loss per unit pathlength becomes negative since the electron can gain energy from the phonons for the "room-temperature" case.

References and Footnotes

†Research sponsored jointly by the Solid State Sciences Directorate, Rome Air Development Center, under Interagency Agreement DOE No. 0226-0226-A1 and the Office of Health and Environmental Research, U.S. Department of Energy, under contract DE-AC05-84OR21400 with Martin Marietta Energy Systems, Inc.

1. W. T. Lynch, *J. Appl. Phys.* 43, 3274 (1972).
2. D. K. Ferry, *Appl. Phys. Lett.* 27, 689 (1975); *J. Appl. Phys.* 50, 1422 (1979).
3. H.-J. Fitting and J.-U. Friemann, *Phys. Stat. Sol. A* 69, 349 (1982).
4. M. V. Fischetti, *Phys. Rev. Lett.* 53, 1755 (1984).
5. M. V. Fischetti, D. J. DiMaria, S. D. Brorson, T. N. Theis, and J. R. Kirtley, *Phys. Rev. B* 31, 8124 (1985).
6. M. Sparks, D. L. Mills, R. Warren, T. Holstein, A. A. Maradudin, L. J. Sham, E. Loh, Jr., and D. F. King, *Phys. Rev. B* 24, 3519 (1981).
7. H. Frölich, *Adv. Phys.* 3, 325 (1954).
8. J. Llacer and E. L. Garwin, *J. Appl. Phys.* 40, 2766 (1969).
9. R. W. G. Wyckoff, "Crystal Structures" (Interscience, New York, 1965).
10. W. G. Spitzer and D. A. Kleinman, *Phys. Rev.* 121, 1324 (1961).
11. Handbook of Chemistry and Physics (CRC Press, Boca Raton, Florida, 1981).

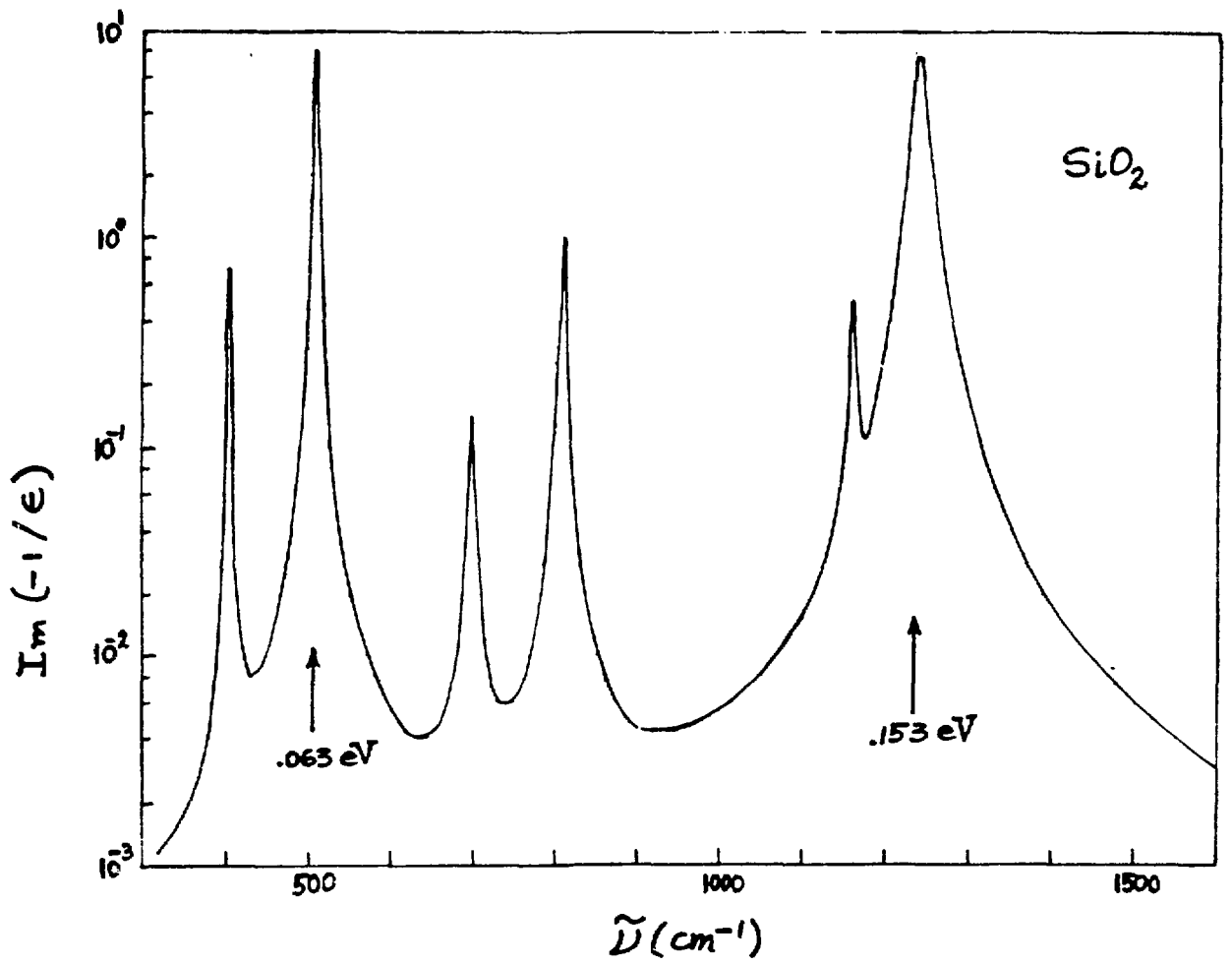


FIG. 1

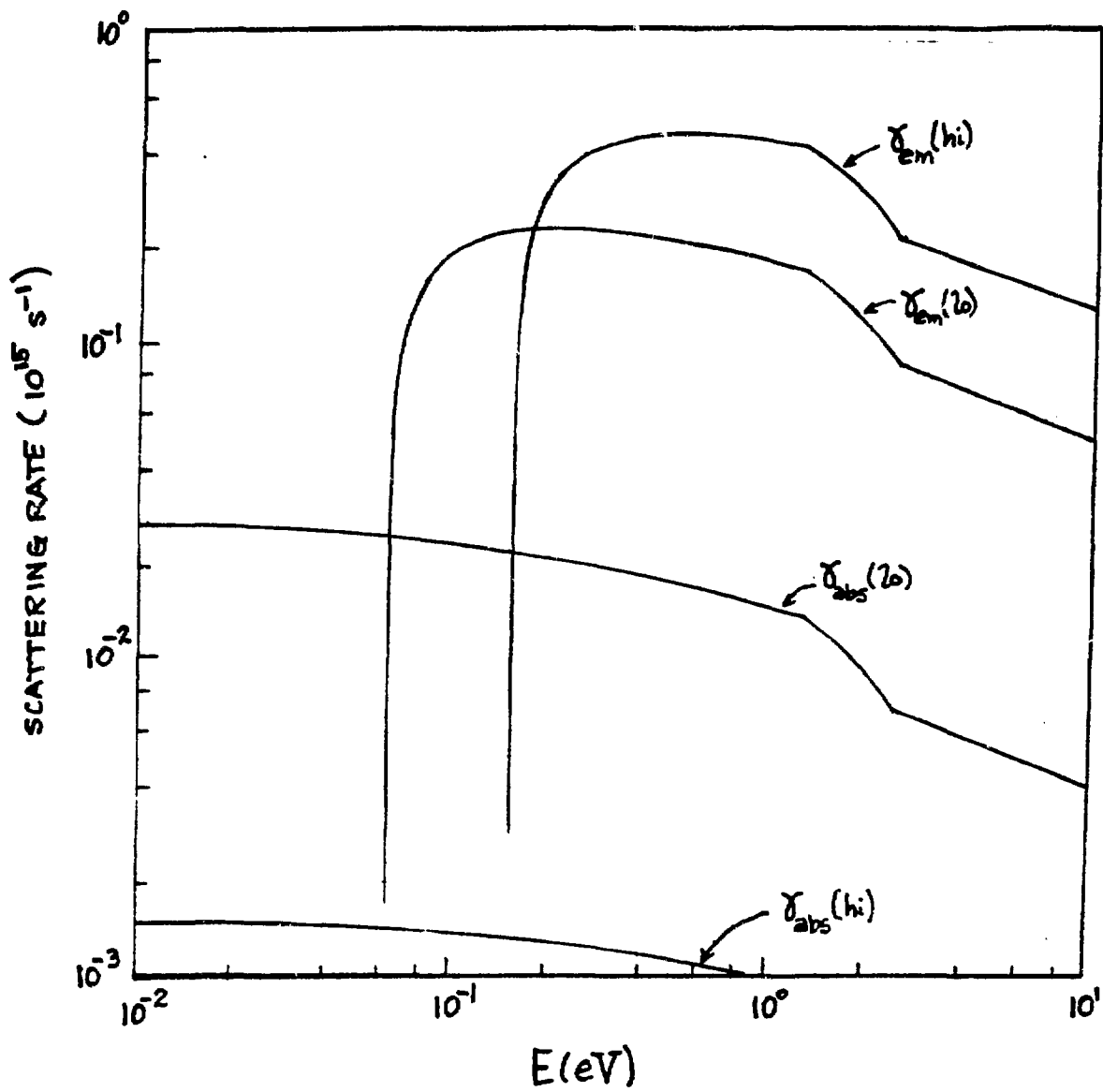


FIG. 2

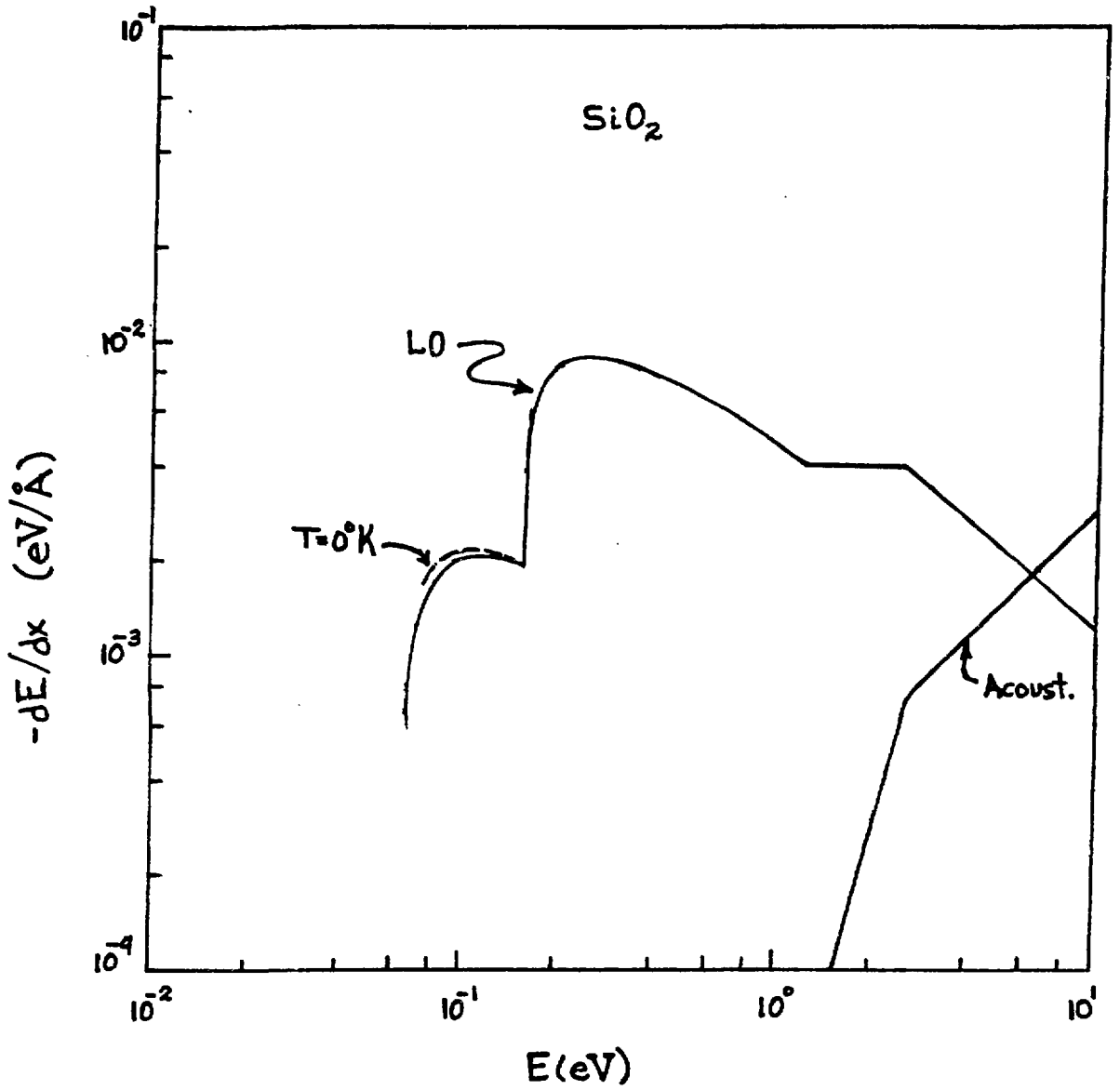


FIG. 3

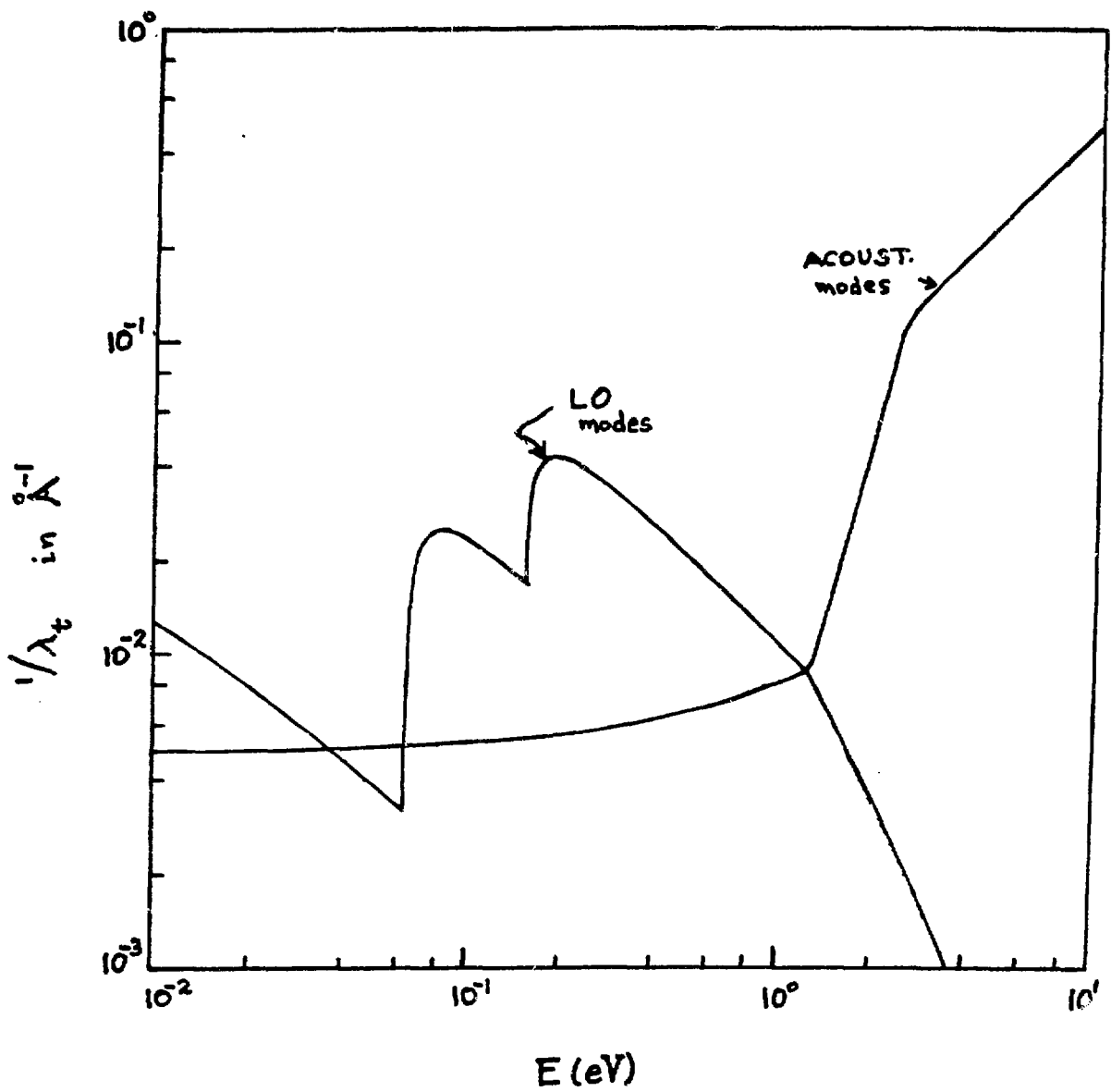


FIG. 4

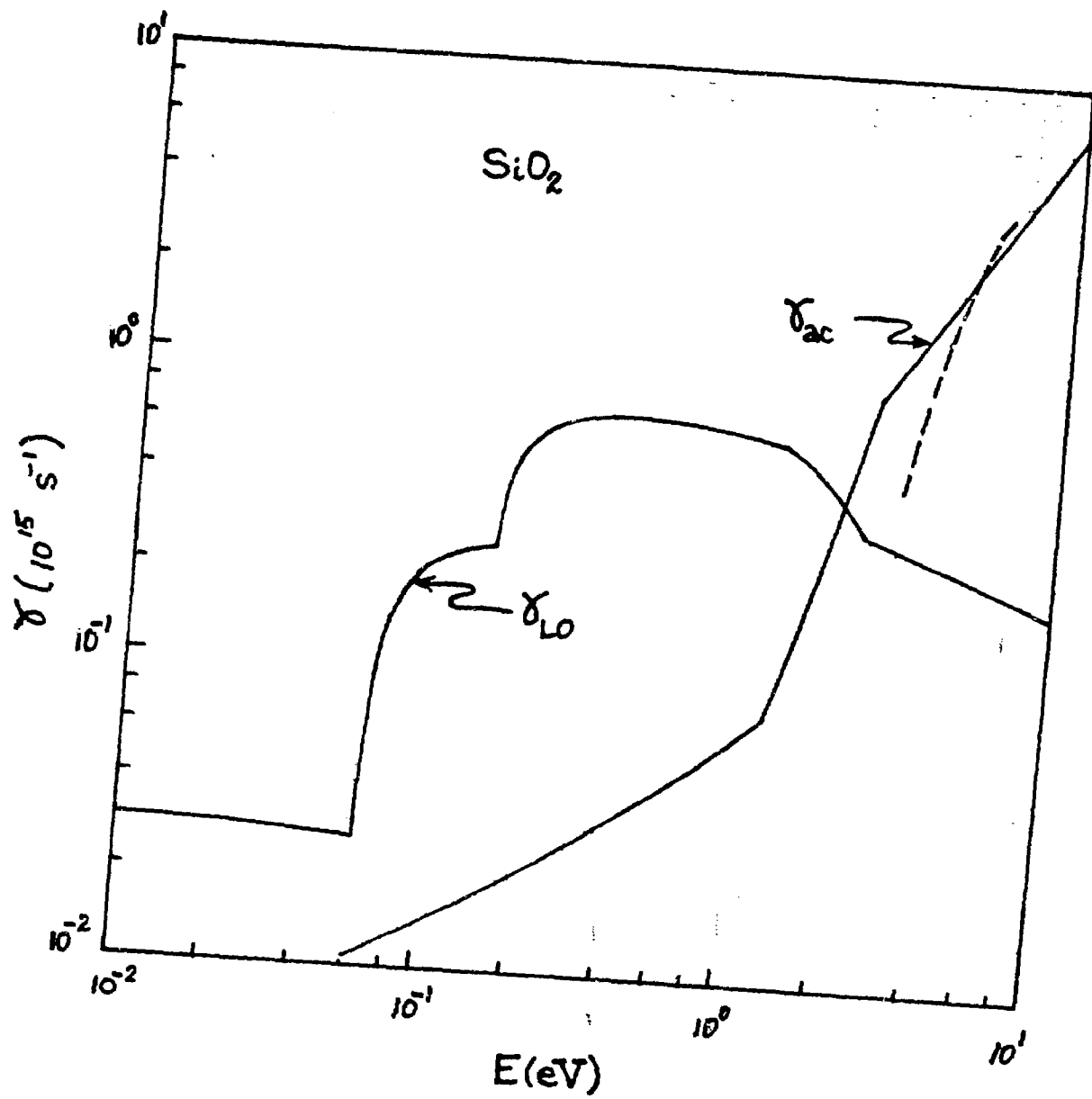
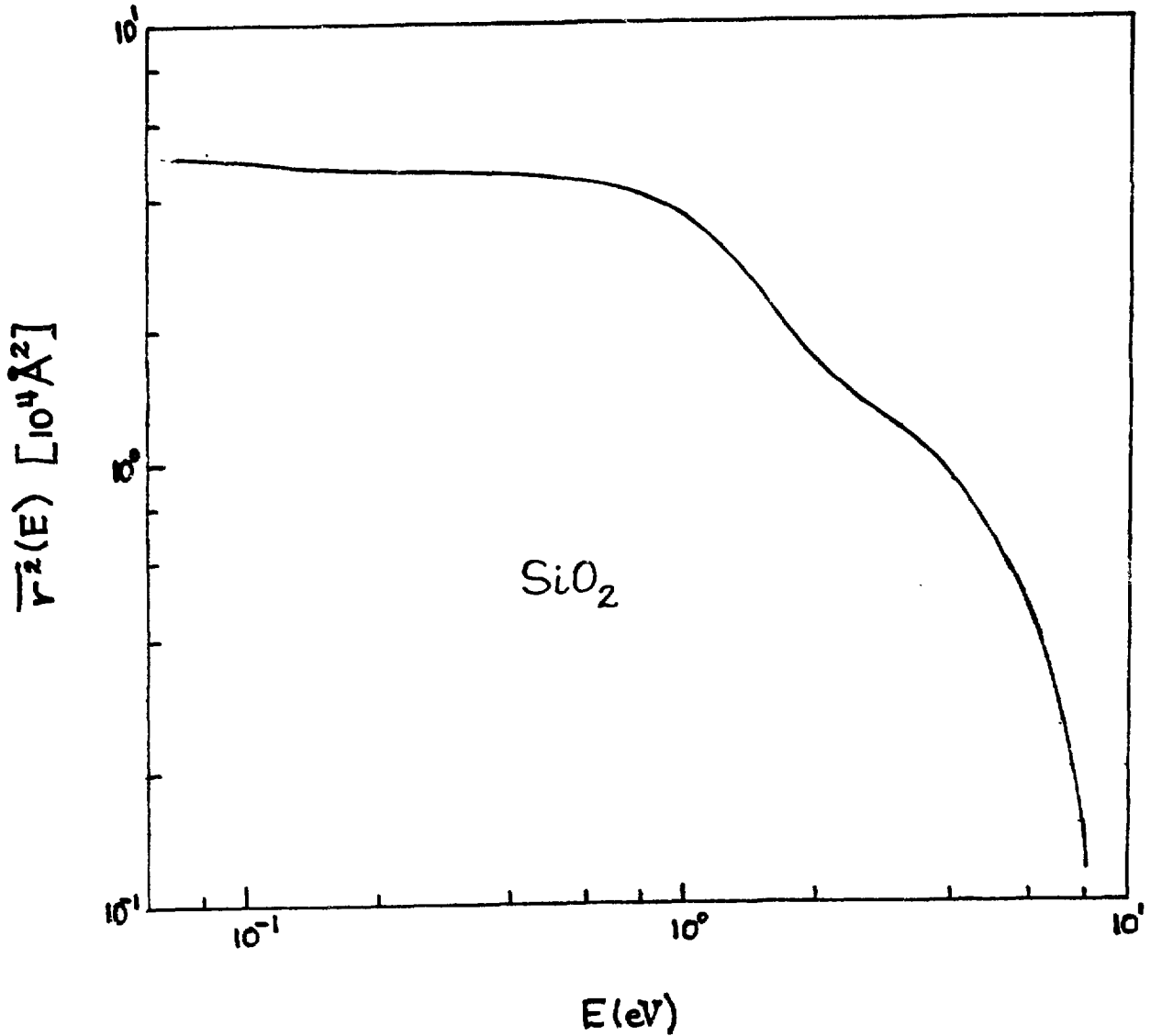


FIG. 5



DISCLAIMER

FIG. 6

This report was prepared as an account of work sponsored by an agency of the United States Government. Neither the United States Government nor any agency thereof, nor any of their employees, makes any warranty, express or implied, or assumes any legal liability or responsibility for the accuracy, completeness, or usefulness of any information, apparatus, product, or process disclosed, or represents that its use would not infringe privately owned rights. Reference herein to any specific commercial product, process, or service by trade name, trademark, manufacturer, or otherwise does not necessarily constitute or imply its endorsement, recommendation, or favoring by the United States Government or any agency thereof. The views and opinions of authors expressed herein do not necessarily state or reflect those of the United States Government or any agency thereof.